

Study On Effectiveness Using Copper Oxide Nanofluid In Shell And Tube Heat Exchanger

Syed Sameer¹, Dr. S.B. Prakash², Ganesha T³, Narayana Swamy G⁴

¹Research Scholar, Department of Mechanical Engineering, VTU RRC Belagavi, Karnataka 590018, India.

²Professor, Department of Mechanical Engineering, VTU CPGS Mysore, Karnataka 570019, India.

³Assistant Professor, Department of Mechanical Engineering, VTU CPGS Mysore, Karnataka 570019, India

⁴Assistant Professor, Department of Mechanical Engineering, CPGS, VIAT, Muddenahalli, Chikkaballapura, Karnataka 562101, India.

¹syedsameer30@gmail.com

Abstract - In different applications, nanofluids have competent heat transfer improvement properties. Nanofluids comprise nanoparticles (1 to 100 nm), dispersed homogeneously and steadily in a base fluid. These dispersed nanoparticles significantly improve the nanofluids' thermal conductivity and convection coefficients, which improves heat transfer. This research article deals on the overall heat transfer coefficient and effectiveness in counter-flow STHE (shell & tube heat exchanger), consisting of 25% baffle cut. The CuO-DW nanofluid was prepared using CuO nanoparticles in DW base fluid by two-step technique at 0.05%, 0.1%, and 0.2% volume fractions. The addition of 0.15% SDBS (Sodium dodecylbenzene sulphonate) as a surfactant enhances dispersed nanoparticles' stability. The thermophysical properties of CuO-DW nanofluid, such as density (ρ), thermal conductivity (k), and dynamic viscosity (μ), increases, but the specific heat (C_p) decreases with an increase in CuO nanoparticles concentration in DW base fluid. The maximum heat exchanger effectiveness was 2.92%, 3.85%, and 5.66% higher than water at a 0.6 lpm mass flow rate for 0.05%, 0.1%, and 0.2% CuO-DW nanofluid volume fractions correspondingly. The actual heat transfer (Q_{actual}), coefficient of overall heat transfer (U_o), and effectiveness (ϵ) of the counter flow STHE are higher compared to water for 0.05%, 0.1%, and 0.2% CuO-DW nanofluid volume fractions as flow rate changes from 0.2 lpm to 1 lpm at $T=80^\circ\text{C}$.

Keywords — CuO (Copper-Oxide) nanoparticles, coefficient of overall heat transfer, effectiveness study, heat exchanger, thermophysical properties, volume fraction.

I. INTRODUCTION

The nanometer particles dispersed into the base fluid instead of the micrometer-sized particles known as nano fluids. The nano fluid usage in practical applications causes two significant challenges like deterioration and

sedimentation [1]. Before using nanofluids in industrial applications, possible risks linked to these concerns must be investigated and resolved. The surfactant materials are used for nanofluids agglomerations control and stability control purposes [2]. Improved thermal efficiency was found for graphene-water nanofluids in vertical STHEs [3]. New research found that nanofluids [4] optimistically substitute traditional coolants. Elias et al. [5] measured STHE's heat output with various performance variables like particle size, particle volume, and particle shape in the waste heat recovery system.

T.P Teng and Y.H Hung et al. [6] have experimentally studied the density and the specific heat of aluminum nanofluid. M Bahiraei et al. [7] simulated W/Al₂O₃ nanofluid heat transfer phenomena in STHE with helical baffles. A two-stage technique [8] for the processing of hybrid nanofluid was implemented. Three separate flow fields [9] were considered, such as laminar, transition, and turbulent flow. TiO₂-W nanofluid tested in a heat exchanger, which increases heat transfer significantly. Jafaar A et al. [10] had evaluated improving heat transfer and stream characteristics related to Al₂O₃/W nanofluid with low flow levels in turbulent flow conditions in horizontal STHE. For almost two decades, nanofluids have been called advanced heat transfer fluids [11] in various applications. Dispersed nanoparticles [12], usually a metal or a metal oxide, significantly raise thermal conductivity in base fluids, raise conduction and convection constants, and allow extra heat transfer in various applications.

This research article focuses on the experimental investigation of the coefficient of overall heat transfer (U_o) and effectiveness (ϵ) of the 25 percent segmental baffle cut counter-flow STHE using CuO nanoparticles at 0.05, 0.1, and 0.2 percentage of volume fractions in the DW base fluid with the addition of 0.15 percent SDBS as a surfactant to



each volume fraction of nanofluid by varying mass flow rate. Theoretical and experimental effectiveness values are compared to evaluate the percentage of error at different nanofluid volume concentrations.

II. MATERIALS AND METHODS

A. Nanoparticles selection



Fig. 1. CuO nanoparticles and SDBS-surfactant.

As figure 1 shows, CuO nanoparticle and SDBS surfactant powder were selected for research work because of their ease of availability, formulation, handling, and improved stability features. While there are several potential features of nanofluids, there are several disadvantages such as clustering, sedimentation, agglomeration, and depletion of thermo-physical properties due to inefficient formulation methods and procedures. The properties and stability of nanofluids were analyzed after preparation and then tested. The use of SDBS surfactant enhances the stability of nanopowder particles in the DW base fluid. Table 1 represents some of the significant properties related to CuO nanopowder particles and water are present. Table 2 provides the details of CuO nanopowder particles used in the study.

Table 1. Significant properties of CuO nanoparticles and water.

Properties	Symbols	S.I. Units	Water	CuO
Density	ρ	(kg/m ³)	1000	6400
Thermal conductivity	k	(W/m-K)	0.613	33
Specific heat	C_p	(J/kg-K)	4187	540
Dynamic viscosity	μ	(Pa-s)	8.9×10^{-4}	-

Table 2. Details of CuO nanoparticles.

Details	Values
Chemical formula	CuO
Color	Black
Physical form	Powder
Morphology	Spherical
True density	6.4 g/cm ³
Bulk density	0.79 g/cm ³
Atomic weight	79.545 per mol
Specific surface area	10-20 m ² /g
Particles size	30-50 nm
Purity	99.98%

B. Nanofluid preparation

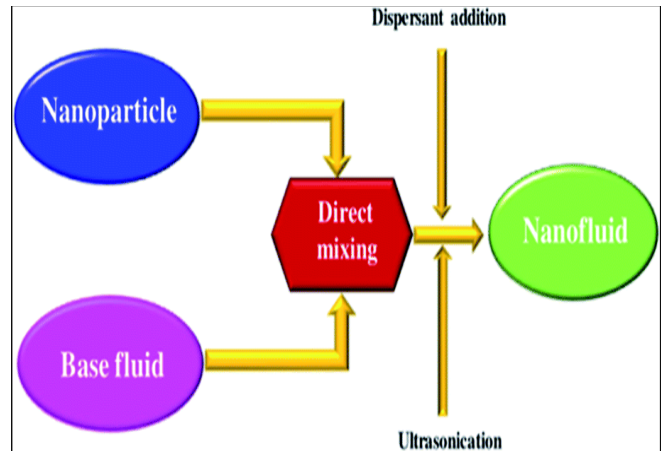


Fig. 2. Block diagram of nanofluid preparation by a two-step technique.

For enhancing heat transfer in nanofluids, oxide nanoparticles need to provide high-volume fractions relative to metal particles in any base fluid to obtain the same level of heat transfer, leading to agglomeration. The objective is to find innovative ways to improve the two-step method of generating wide-ranging nanofluids without agglomeration. These nanofluids are not durable, but they can increase if pH is controlled or surfactants are applied. The two-stage procedure performs well for oxide nanoparticles and is unsuccessful for metallic nanoparticles.

The CuO nanoparticles are used in this research to prepare nanofluids with base fluid DW. The CuO nanoparticles (particle size average 30 to 50 nm and 99.9 percent pure) from Platonic nanotech Pvt Ltd, Jharkhand,

India were commercially purchased. As shown in Fig.2, the nanofluids prepared using the probe sonicator with a two-step technique. The nanoparticles scattered ultrasonically in the DW base fluid. The CuO-DW nanofluid prepared at 0.05%, 0.1%, and 0.2% volume fractions. The addition of 0.15% SDBS as a surfactant to each sample with 90-minutes and above ultrasonication provides increased durability and stability for CuO-DW nanofluid.

C. Stability check



Fig. 3. Stability check for CuO-DW nanofluid by observation.

The long-term stability of suspended nanoparticles is most significant in various applications. A stability check was conducted with a small sample of each nanofluid for 0.05%, 0.1%, and 0.2% CuO-DW nanofluid volume fractions. It has been observed mechanically to identify sedimentation of the CuO nanopowder particles in the DW base fluid. The CuO nanopowder particles used in this test do not undergo sedimentation for one day in all three samples. The addition of SDBS as a dispersant agent to each volume fraction of nanofluids by 0.15 percent provides enhanced stability.

An image was captured after one day, seven days, and fifteen days after the preparation of samples, as shown in Fig. 3. It has been observed that even after 24 hours, there was no sedimentation in the samples. Hence all three samples of nanofluid are assumed to be stable. After seven days, the nanoparticles steadily settle in the top layers, and we can find this in the middle layers after fifteen days. However, over time due to gravitational effects, nanoparticle sediment and stability equilibrium gradually disappear.

III. EXPERIMENTAL SETUP



Fig. 4. STHE experimental test-rig.

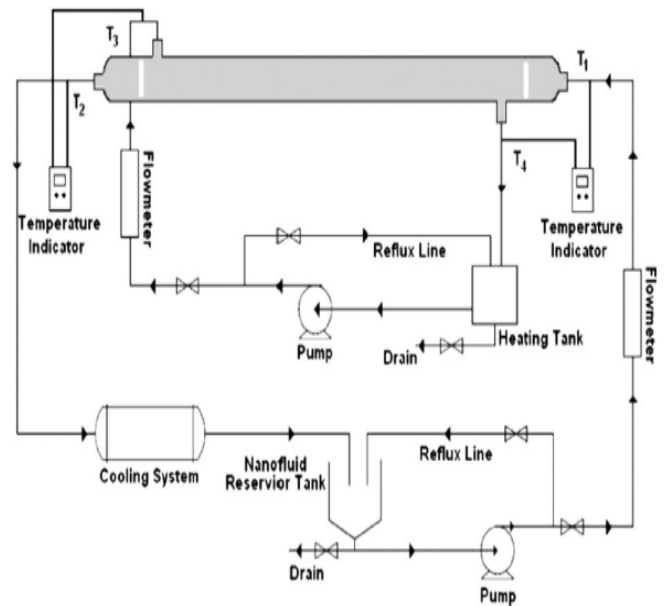


Fig. 5. Line diagram of the STHE test-rig.

The latest test rig consists of an input and output pump, 10-liter capacity 4 tanks, a water heating coil, STHE with thermocouples, and segmental baffles, as shown in figures 4 and 5. Thermocouples 1 and 2 measure the cold fluid (CuO-DW nanofluid) inlet and outlet temperatures, and thermocouples 3 and 4 are used to assess hot fluid (W) entry

and exit temperatures. In the shell, five 25 percent cut segmental baffles were used to create turbulent velocity. The heat exchanger was insulated with tape to avoid heat loss to the surroundings.

The device safeguarded by moving the water through the test-rig to achieve improved effectiveness. CuO-DW nanofluid has been used to extract heat from the hot fluid (i.e., water) at various flow rates of cold nanofluid for counter flow variation of different volume fractions. It helps to analyze the impact of nanoparticles' concentration on heat exchanger effectiveness (ϵ) for overall performance improvement. The details of the experimental arrangement of the test rig, as shown in Table 3.

Table. 3. Details of the experimental arrangement

Details	Values
Tube arrangement	Triangular pitch
Outside shell diameter, (D_o)	63mm
Inside shell diameter, (D_i)	60mm
Baffle cut in %	25%
Type	Single-pass
Tube outer-diameter, (d_o)	22mm
Tube inner-diameter, (d_i)	20mm
Number of tubes, (N)	3
Tube length, (l)	500mm
The spacing of baffles, (B)	83.3mm
Tube Pitch, (p_i)	27.5mm
The capacity of each Rotameter	0 to 1 lpm
Type of thermocouples	PT-100
Tube material	Copper
Shell material	Stainless steel
Number of baffles (N_b)	5
Thickness of baffles	3mm

IV. PROCEDURE FOR ESTIMATION OF EFFECTIVENESS

A. Equations used for properties estimation

The volume fraction [8],[11] percentage is determined using equation (1).

$$\% \text{ of Volume fraction } (\phi) = \left[\frac{\frac{W_{np}}{\rho_{np}}}{\frac{W_{np}}{\rho_{np}} + \frac{W_{bf}}{\rho_{bf}}} \right] \times 100 \quad (1)$$

For the estimate of density [13] and specific heat [14] for all volume fractions, Pak & Cho (1998) developed the (2) and

(3) nanofluid equations by using the theory of mixture.

$$\rho_{nf} = [(\phi \times \rho_{np}) + ((1 - \phi) \times \rho_{bf})] \quad (2)$$

$$C_{p(nf)} = [(\phi \times C_{p(np)}) + ((1 - \phi) \times C_{p(bf)})] \quad (3)$$

For the evaluation of thermal-conductivity (k_{nf}) in nanofluids, Maxwell [3] formulated equation (4) used.

$$k_{nf} = k_{bf} \left[\frac{k_{np} + 2k_{bf} + 2\phi(k_{np} - k_{bf})}{k_{np} + 2k_{bf} - \phi(k_{np} - k_{bf})} \right] \quad (4)$$

In the nanofluids' viscosity calculation, Drew and Passman [10] proposed the renowned equation (5) established by Einstein, which is suitable for the volume fraction of less than 5%.

$$\mu_{nf} = [1 + (2.5 \times \phi)] \mu_{bf} \quad (5)$$

B. Heat exchangers effectiveness analysis

The coefficient of overall heat transfer (U_o) and effectiveness (ϵ) of the STHE are calculated by employing the succeeding equations [15], [16].

$$U_o = \left[\frac{Q}{A \times LMTD} \right] \quad (6)$$

The area of heat transfer in m^2 is

$$A = \pi d_o l \times n \quad (7)$$

Actual heat transfer (Q_{actual}) is obtained [3] by

$$Q_{actual} = [V(\rho C_p)_{nf} (T_{h1} - T_{h2})] \quad (8)$$

LMTD (Logarithmic Mean Temperature Difference) is given by

$$LMTD = \left[\frac{(\Delta T_1 - \Delta T_2)}{\ln \left(\frac{\Delta T_1}{\Delta T_2} \right)} \right] \quad (9)$$

Where, $\Delta T_1 = [T_{h1} - T_{c1}]$ and $\Delta T_2 = [T_{h2} - T_{c2}]$ for parallel-flow

And $\Delta T_1 = [T_{h1} - T_{c2}]$ and $\Delta T_2 = [T_{h2} - T_{c1}]$ for counter-flow

The effectiveness is defined as

$$\epsilon = \frac{Q}{Q_{max}} \quad (10)$$

$$\epsilon = \left[\frac{Q}{C_{min} (T_{h1} - T_{c1})} \right] \quad (11)$$

Heat capacities associated with hot and cold fluids determined from equations (12) and (13).

$$C_h = m_h C_{ph} \quad (12)$$

$$C_c = m_c C_{pc} \quad (13)$$

Among the values of C_h and C_c , a lower value is considered as C_{min} .

If $C_h < C_c$, effectiveness (ϵ) [16] is

$$\epsilon_{Exp} = \frac{[Th_1 - Th_2]}{[Th_1 - Tc_2]} \quad (14)$$

If $C_c < C_h$, effectiveness (ϵ) [16] is

$$\epsilon_{Exp} = \frac{[Tc_2 - Tc_1]}{[Th_1 - Tc_1]} \quad (15)$$

Theoretical effectiveness for single-shell pass was calculated by using the following equation [16].

$$\epsilon_1 = 2 \left\{ \left[1 + C + (1 + C^2)^{0.5} \right] X \frac{1 + \exp[-NTU(1 + C^2)^{0.5}]}{1 - \exp[-NTU(1 + C^2)^{0.5}]} \right\}^{-1} \quad (16)$$

For n shell passes, theoretical effectiveness [16] is calculated by

$$\epsilon_{The} = \left\{ \frac{[(1 - \epsilon_1 C)/(1 - \epsilon_1)]^n - 1}{[(1 - \epsilon_1 C)/(1 - \epsilon_1)]^n - C} \right\} \quad (17)$$

The percentage of error ineffectiveness was calculated by using the following equation.

$$\% \text{ of error in effectiveness } (\epsilon) = \left(\frac{\epsilon_{The} - \epsilon_{Exp}}{\epsilon_{The}} \right) X 100 \quad (18)$$

V. RESULTS AND DISCUSSION

A. CuO nanoparticles volume fraction (ϕ) effect on the nanofluid thermo-physical properties

Table. 4. Calculated properties of CuO-DW nanofluid at different volume fractions.

Nanofluid volume fractions	Density (kg/m ³)	Specific heat (J/kg-K)	Thermal conductivity (W/m-K)	Dynamic viscosity (Pa-s)
0.05% CuO-DW	1270	4004.6	0.7043	0.001001
0.1% CuO-DW	1540	3822.3	0.8052	0.001112
0.15% CuO-DW	1810	3639.9	0.9172	0.001223
0.2% CuO-DW	2080	3457.6	1.0422	0.001335

Table.4 represents density (ρ), thermal conductivity (k), and dynamic viscosity (μ) of the CuO-DW nanofluid increases from 21.25% to 51.92%, 12.96% to 41.18%, and 11% to 33.58% as the percentage of volume fraction (ϕ) of CuO nanopowder particles increases from 0.05% to 0.2% compared to base fluid DW. But specific heat (cp) of CuO-DW nanofluid reduces from 4.35% to 17.42% as the percentage of volume fraction (ϕ) increases from 0.05% to 0.2% in the DW base fluid.

B. Influence of m_c on the Q_{actual} in STHE

The actual heat transfer was tested for several experiments in a horizontal STHE with the counter-flow variations. The Q_{actual} was determined primarily for hot water to cold water. Hot water circulated at temperature 80°C through the tubes. The exact amount of heat transfer was calculated by maintaining a steady flow rate of hot fluid (Water) at 0.3 lpm and varying cold fluid (CuO-DW) flow rates at 0.2, 0.4, 0.6, 0.8, and 1 lpm.

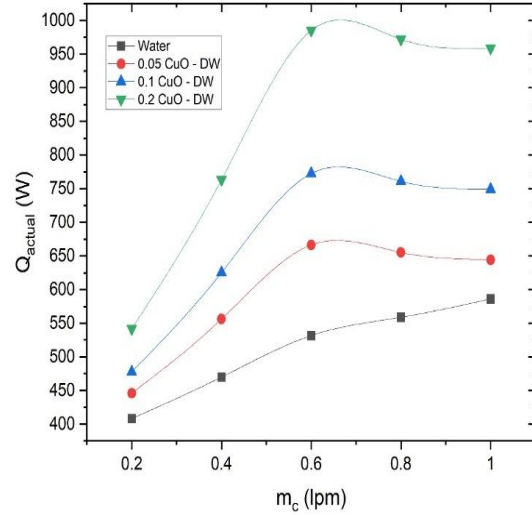


Fig. 6. Influence of mass flow (m_c) rate on Q_{actual} at $T=80^\circ\text{C}$.

At 0.2 lpm, CuO-DW nanofluid provides 8.45%, 14.57%, and 24.65% higher actual heat transfer than water (W) for 0.05%, 0.1%, and 0.2% fractions of CuO nanopowder particles with base fluid DW, correspondingly. Similarly, at 0.6 lpm, it gives 20.18%, 31.18%, and 46.03% actual heat transfer higher compared to water for 0.05%, 0.1%, and 0.2% volume fractions. Also, at 0.1 lpm, CuO-DW nanofluid provides 9%, 21.75%, and 38.87% more heat transfer than water (W) for 0.05%, 0.1%, and 0.2% volume fractions CuO nanopowder particles correspondingly. A 0.6 lpm provides maximum actual heat transfer than water for all three different CuO-DW nanofluid concentrations at temperature $T=80^\circ\text{C}$. Therefore CuO-DW nanofluid showed an increase in actual heat transfer than water at a 0.05%, 0.1%, and 0.2% volume concentration of CuO nanopowder particles in the DW base fluid during counter-flow.

C. Influence of m_c on the U_o in STHE

Fig. 7. (a) and (b) denote the influence of m_c on the U_o at $T=80^\circ\text{C}$ during counter-flow for 0.05%, 0.1%, and 0.2% CuO nanoparticles volume fractions. The CuO-DW nanofluid was used as a cold fluid within the test rig's shell, and tube-side hot water circulated at 80°C inlet temperature.

The results show that the U_o value rises as the nanofluid flow rate rises. The maximum U_o values were found to be at 0.6 lpm flow amount of CuO-DW nanofluid. At 0.6 lpm and temperature $T=80^{\circ}\text{C}$, the U_o values are 11.3%, 18.26%, and 29.34% higher than water for 0.05%, 0.1%, and 0.2% CuO-DW nanofluid volume fractions correspondingly, during counter-flow arrangement in STHE.

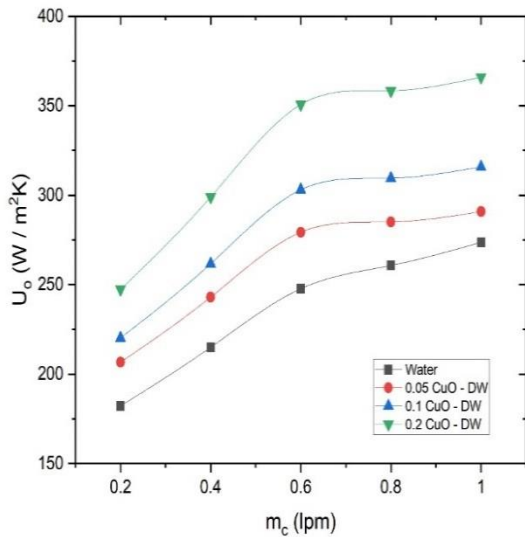


Fig. (a).

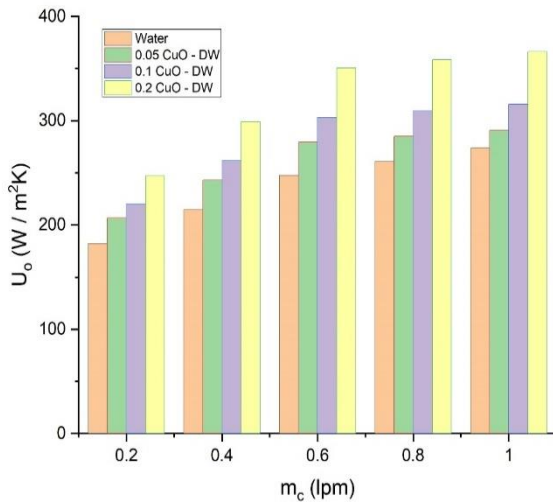


Fig. (b).

Fig. 7. (a) and (b), Influence of mass flow (m_c) on the coefficient of overall heat transfer (U_o) at $T=80^{\circ}\text{C}$.

D. Outcome of effectiveness (ϵ) with mass flow (m_c) rate

Fig. 8 (a) and (b) indicate the result of the CuO-DW nanofluid mass flow rate on heat exchanger effectiveness for various volume fractions of CuO nanoparticles (0.05%, 0.1%, and 0.2%). The outcomes show that as the flow rate of nanofluid rises, then STHE effectiveness also rises. The CuO-DW nanofluid's 0.2% volume fraction provides improved performance compared to other 0.1%, 0.05% volume fractions of CuO-DW nanofluid and water. Hence, the STHE maximum effectiveness values were 2.92%, 3.85%, and 5.66% higher than water for 0.05%, 0.1%, and 0.2% CuO-DW nanofluid volume fractions at flow rate 0.6 lpm and temperature $T=80^{\circ}\text{C}$ during counter-flow.

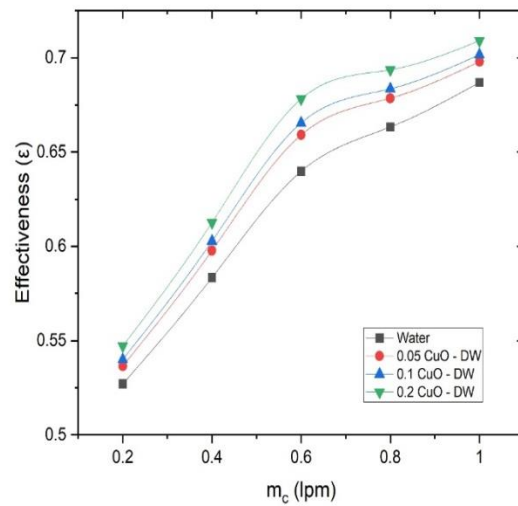


Fig. (a)

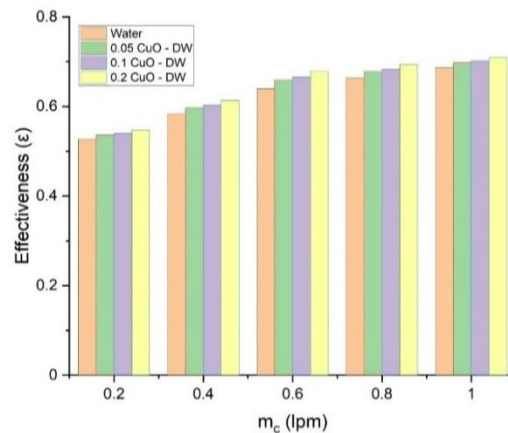


Fig. (b).

Fig. 8. (a) and (b), Effectiveness (ϵ) variations with mass flow rate (m_c) at $T=80^{\circ}\text{C}$.

E. Assessment among experimental and theoretical effectiveness values

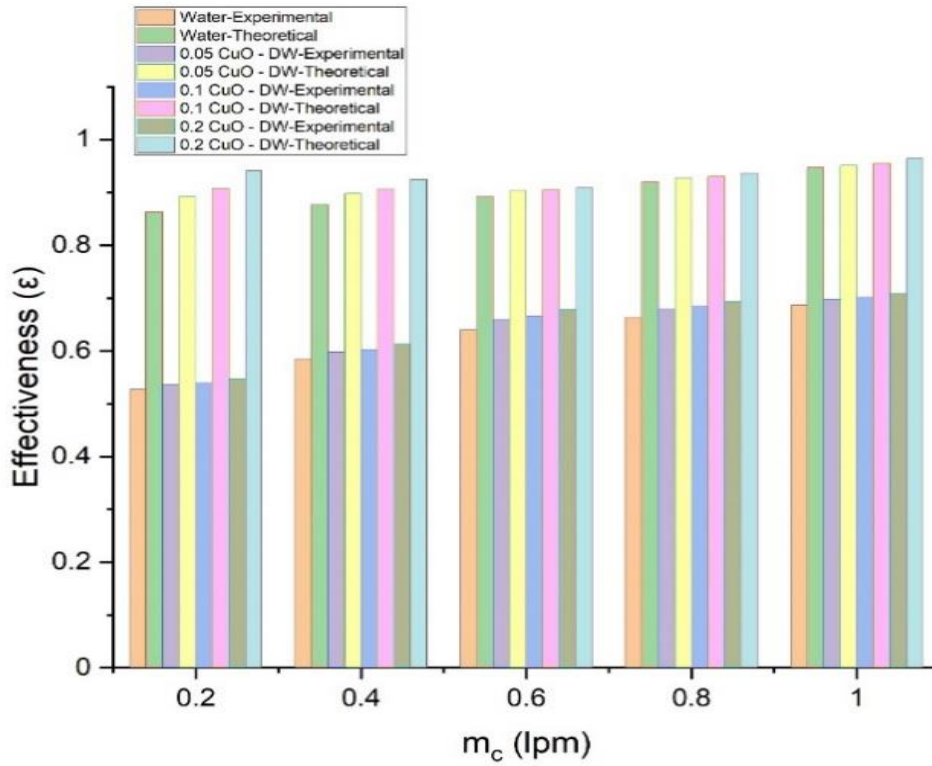


Fig. 9. Assessment among experimental and theoretical effectiveness values (ϵ) at $T=80^{\circ}\text{C}$ for water and CuO-DW nanofluid.

It is a known fact that any theoretically calculated results should be higher than the experimentally evaluated results. Because during theoretical calculations, ideal conditions are to be considered by neglecting certain factors with assumptions. Therefore, the theoretical effectiveness values of STHE always greater than experimental values for any fluid medium. As the flow proportion increases, the effectiveness of the STHE also increases. Initially, at 0.2 lpm of nanofluid flow rate, the difference between theoretical and experimental effectiveness values maximum due to nanofluid's lower flow rate. As the nanofluid flow rate rises to 1 lpm, the variation between theoretical and experimental effectiveness reaches the minimum value. Also, it evident that an increasing volume fraction of CuO nanopowder particles in the DW base fluid increases the STHE effectiveness. Hence 0.2 percent volume concentration of CuO-DW nanofluid shown the minimum difference between theoretical and experimental values as flow rate changes from 0.2 lpm to 1 lpm as revealed in Fig. 9.

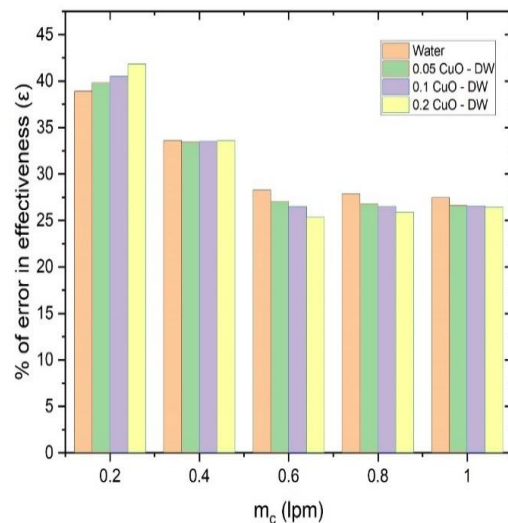


Fig. 10. % of error in effectiveness values (ϵ) at $T=80^{\circ}\text{C}$ for CuO-DW nanofluid.

Fig. 10 denotes the percentage of error in effectiveness between theoretical and experimental values with a cold CuO-DW nanofluid flow rate. As the flow changes from 0.2 lpm to 1 lpm, the % of error declines from maximum to minimum due to an increase in experimental effectiveness values during counter flow arrangement of STHE at T=80°C temperature of the hot fluid (water). Therefore 0.05%, 0.1%, and 0.2% CuO-DW nanofluid volume fractions showed the minimum percentage of error compared to water. The flow proportion progressed from 0.2 lpm to 1 lpm for counter-flow arrangement STHE setup.

VI. CONCLUSIONS

The thermophysical properties of CuO-DW nanofluid at 0.05%, 0.1%, and 0.2% volume concentrations calculated using suitable equations. The effect of CuO nanoparticles' concentrations on the effectiveness was studied extensively. The following outlines were drawn:

1. The density (ρ), thermal conductivity (k), and dynamic viscosity (μ) of the CuO-DW nanofluid increase with a rise in the volume fraction of CuO nanopowder particles with DW base fluid, but the specific heat (c_p) of nanofluid declining with increasing volume fraction in the DW base fluid.
2. The actual heat transfer (Q_{actual}), coefficient of overall heat transfer (U_o), and effectiveness (ϵ) of the counter-flow STHE for several volume fractions of CuO-DW nanofluid increases compared to water as flow rate changes 0.2 lpm to 1 lpm at T=80°C.
3. The maximum improvement of U_o (coefficient of overall heat-transfer) value was 11.3%, 18.26%, 29.34% higher than water for volume concentrations 0.05%, 0.1%, and 0.2% CuO-DW nanofluid respectively at 0.6 lpm mass flow rate and temperature T=80°C during counter flow variation.
4. The maximum STHE effectiveness values were 2.92%, 3.85%, and 5.66% higher than water for 0.05%, 0.1%, and 0.2% CuO-DW nanofluid volume concentrations the flow rate 0.6 lpm and temperature T=80°C during counter-flow.
5. In heat exchangers, always theoretical effectiveness values higher than experimental effectiveness values. But the percentage of error between these values decreases as the difference between these values reduces and vice-versa.

APPENDIX A

Nomenclature

General

A	Surface area; (m ²)
C_c	Cold-fluid heat capacity; (W/K)
C_h	Hot-fluid heat capacity; (W/K)
C_p	Specific heat at constant pressure; (J/kg-K)
C_v	Specific heat at constant volume; (J/kg-K)

$C_{p(nf)}$	Specific heat of nanofluid; (J/kg-K)
$C_{p(np)}$	Specific heat of nanoparticles; (J/kg-K)
$C_{p(bf)}$	Specific heat of base-fluid; (J/kg-K)
D_s	Inner-diameter of shell; (m)
d_o	Outer-diameter of tube; (m)
k	Thermal conductivity; (W/m-K)
k_{bf}	Thermal conductivity of base-fluid; (W/m-K)
k_{nf}	Thermal conductivity of nanofluid; (W/m-K)
k_{np}	Thermal conductivity of nanoparticles; (W/m-K)
l	Tube length; (m)
m_c	Mass flow rate of cold-fluid; (kg/s)
m_h	Mass flow rate of hot-fluid; (kg/s)
n	Number of tubes; (-)
N_b	Number of baffles; (-)
Q_{actual}	Actual heat-transfer rate; (W)
Q_{max}	Maximum possible heat-transfer; (W)
T	Temperature; (K)
T_{c1}	Temperature of cold-fluid at inlet; (K)
T_{c2}	Temperature of cold-fluid at outlet; (K)
T_{h1}	Temperature of hot-fluid at inlet; (K)
T_{h2}	Temperature of hot-fluid at outlet; (K)
ΔT_1	Temperature difference at inlet; (K)
ΔT_2	Temperature difference at outlet; (K)
$LMTD$	Logarithmic mean temperature difference; (-)
U_o	Overall heat transfer coefficient; (W/m ² -K)
ρ_{nf}	Density of nanofluid; (kg/m ³)
ρ_{bf}	Density of base-fluid; (kg/m ³)
ρ_{np}	Density of nanoparticle; (kg/m ³)
μ_{nf}	Dynamic viscosity of nanofluid; (Pa-s)
μ_{bf}	Dynamic viscosity of base-fluid; (Pa-s)

Abbreviations

W	Water; (-)
DW	Distilled water; (-)
lpm	Liters per minute; (-)
SSA	Specific surface area; (m ² /g)
$STHE$	Shell and tube heat exchanger; (-)
$SDBS$	Sodium dodecylbenzene sulfonate; (-)

Greek symbols

ϵ	Effectiveness; (-)
μ	Dynamic viscosity; (Pa-s)
ρ	Density; (kg/m ³)
ϕ	The volume concentration of nanofluid; (%)

Subscripts

b	baffle
c	Cold
h	Hot
1	Inlet
2	Outlet
bf	Base fluid
nf	Nanofluid
np	Nanoparticles

ACKNOWLEDGMENT

This research work has not received any funding from any agencies/boards. The authors are grateful to the authorities of Visvesvaraya Technological University, CPGS- Mysore & Muddenahalli, for their continuous support and encouragement for the smooth conduction of the research work.

REFERENCES

- [1] Jehhef K.A, Al Abas Siba M.A. Effect of Surfactant Addition on the Nanofluids Properties: a Review. *Acta Mech Malaysia* 2019;2:01–19. <https://doi.org/10.26480/amm.02.2019.01.19>.
- [2] Barzegarian R, Aloueyan A, Yousefi T. Thermal performance augmentation using water-based Al_2O_3 -gamma nanofluid in a horizontal shell and tube heat exchanger under forced circulation. *Int Commun Heat Mass Transf* 2017;86:52–9. <https://doi.org/10.1016/j.icheatmasstransfer.2017.05.021>.
- [3] Fares M, AL-Mayyahi M, AL-Saad M. Heat transfer analysis of a shell and tube heat exchanger operated with graphene nanofluids. *Case Stud Therm Eng* 2020;18:100584. <https://doi.org/10.1016/j.csite.2020.100584>.
- [4] Shahrul IM, Mahbulul IM, Saidur R, Khaleduzzaman SS. Numerical Heat Transfer, Part A : Applications : An International Journal of Computation and Methodology Effectiveness Study of a Shell and Tube Heat Exchanger Operated with Nanofluids at Different Mass Flow Rates 2014:37–41. <https://doi.org/10.1080/10407782.2013.846196>.
- [5] Elias MM, Shahrul IM, Mahbulul IM, Saidur R, Rahim NA. International Journal of Heat and Mass Transfer Effect of different nanoparticle shapes on shell and tube heat exchanger using different baffle angles and operated with nanofluid. *Int J Heat Mass Transf* 2014;70:289–97. <https://doi.org/10.1016/j.ijheatmasstransfer.2013.11.018>.
- [6] Teng TP, Hung YH. Estimation and experimental study of the density and specific heat for alumina nanofluid. *J Exp Nanosci* 2014;9:707–18. <https://doi.org/10.1080/17458080.2012.696219>.
- [7] Bahiraei M, Hosseinalipour SM, Saeedan M. Prediction of Nusselt Number and Friction Factor of Water- Al_2O_3 Nanofluid Flow in Shell-and-Tube Heat Exchanger with Helical Baffles, 2015;6445. <https://doi.org/10.1080/00986445.2013.840828>.
- [8] Senthilraja S, Vijayakumar K, Gangadevi R. A comparative study on thermal conductivity of Al_2O_3 /water, CuO/water, and Al_2O_3 -CuO/water nanofluids. *Dig J Nanomater Biostructures* 2015;10:1449–58.
- [9] Subramanian R, Senthil Kumar A, Vinayagar K, Muthusamy C. Experimental analyses on heat transfer performance of TiO_2 -water nanofluid in the double-pipe counter-flow heat exchanger for various flow regimes. *J Therm Anal Calorim* 2020;140:603–12. <https://doi.org/10.1007/s10973-019-08887-1>.
- [10] Albadr J, Tayal S, Alasadi M. Case Studies in Thermal Engineering Heat transfer through heat exchanger using Al_2O_3 nanofluid at different concentrations. *Case Stud Therm Eng* 2013;1:38–44. <https://doi.org/10.1016/j.csite.2013.08.004>.
- [11] Sonawane SS, Khedkar RS, Wasewar KL. Study on concentric tube heat exchanger heat transfer performance using Al_2O_3 -water-based nanofluids. *Int Commun Heat Mass Transf* 2013;49:60–8. <https://doi.org/10.1016/j.icheatmasstransfer.2013.10.001>.
- [12] Humnic G, Humnic A. Application of nanofluids in heat exchangers : A review. *Renew Sustain Energy Rev* 2012;16:5625–38. <https://doi.org/10.1016/j.rser.2012.05.023>.
- [13] Vajjha RS, Das DK, Mahagaonkar BM. Density measurement of different nanofluids and their comparison with theory. *Pet Sci Technol* 2009;27:612–24. <https://doi.org/10.1080/10916460701857714>.
- [14] Elias MM, Miqdad M, Mahbulul IM, Saidur R, Kamalisarvestani M, Sohel MR, et al. effect of nanoparticle shape on the heat transfer and thermodynamic performance of a shell and tube heat exchanger ☆. *Int Commun Heat Mass Transf* 2013;44:93–9. <https://doi.org/10.1016/j.icheatmasstransfer.2013.03.014>.
- [15] Ozisik M. *Necati-Heat Transfer_ A Basic Approach*-McGraw-Hill Book Company (1985).pdf n.d.
- [16] B. Sreenivasa Reddy and K. Hemachandra Reddy. *Thermal Engineering Data Handbook – Revised Edition* 2012; p. 150-163. \
- [17] Naman Jinsiwale, Prof. Vishal Achwal "Heat Transfer Enhancement in Automobile Radiator Using Nanofluids: A Review", *International Journal of Engineering Trends and Technology (IJETT)*, V55(2),68-74 January 2018. ISSN:2231-5381.